Astron. Astrophys. 331, 1099–1102 (1998)

ASTRONOMY
AND
ASTROPHYSICS

Magnetic ionization fronts

I. Parallel magnetic fields

M.P. Redman[1,2], **R.J.R. Williams**[2], **J.E. Dyson**[2], **T.W. Hartquist**[3], **and B.R. Fernandez**[1]

[1] Department of Physics and Astronomy, University of Manchester, UK
[2] Department of Physics and Astronomy, University of Leeds, UK
[3] Max-Planck-Institut für extraterrestrische Physik, D-85740 Garching, Germany

Received 16 January 1997 / Accepted 24 October 1997

Abstract. We solve the continuity equations across an ionization front. By including a plane parallel magnetic field we find significant differences in the allowed velocities of the R- and D-type solutions between the magnetized and non-magnetized cases. These results may have implications for the study of ionization bounded diffuse sources where a moderate or strong magnetic field is expected.

Key words: MHD – ISM: clouds – H II regions – ISM: magnetic fields

1. Introduction

Ionization fronts mark the transition from neutral to ionized gas and are found, for example, at the edges of H II regions, around photoionized clumps and in stellar wind bubbles. Ionization front (IF) structure and propagation were first systematically studied in the classic papers of Kahn (1954), Axford (1961) and Goldsworthy (1961). The standard classification into R-type ('rarefied') and D-type ('dense') IFs was introduced by Kahn (1954). Yorke (1986) has reviewed work on H II region evolution and dynamics up to that date. In such studies the neutral gas density is assumed to be either uniform or to vary smoothly.

However, practically all diffuse astronomical sources are clumpy; this includes Wolf-Rayet and planetary nebulæ, molecular clouds and active galactic nuclei. Hartquist & Dyson (1993) and Dyson et al. (1997) have reviewed the response of clumpy sources to mass, momentum and energy input. In many sources, energy input by ionizing photons is important. Clumps photoionized by an external radiation field lose their heated surfaces by simple expansion, provided that their surface pressure exceeds that of their surroundings (Dyson 1968, 1994; Kahn 1969; Bertoldi & McKee 1990). Mass injection from photoionized clumps has been suggested as the source of the ionized material in ultracompact H II regions (Dyson 1994; Dyson et al. 1995; Redman et al. 1996; Williams et al. 1996; Lizano & Canto 1995; Lizano et al. 1996). The photoevaporation of neutral material is graphically shown in the HST images of the elephant-trunk structures in M16 (Hester et al. 1996) and the cometary knots in the Helix nebula (O'Dell & Handron 1996).

The evaporation rates and lifetimes of photoionized clumps are central to the clumpy UCHIIR models. The studies above deal with the photoionization of non-magnetized, isothermal, self-gravitating clumps. All these assumptions are questionable. The statistical studies of Myers et al. (1995) and Myers & Khersonsky (1995) show that the ratio between magnetic and thermal pressure may be of the order ten or so in diffuse neutral clouds and up to an order of magnitude higher than that in clumps like those identified by Williams et al (1995) from CO maps of the Rosette Molecular Cloud. The ratios of the magnetic pressure to thermal pressure in some dense cores associated with low mass star formation are each only of the order of a few, but, after mass loss from a high mass star begins in a region, such cores can be compressed, and this might lead to increases of the ratios. Magnetic fields have been included in the study of shock fronts (see e.g. Draine & McKee 1993) but the effect on the different types of ionization front has not been described.

Ideally, the effects of turbulence in the ambient medium on the propagation of an ionization front should be considered. We intend to address this point in future papers. However, there are situations in which the ratios of the magnetic pressure to thermal pressure and of the magnetic pressure to the turbulent pressure could be high; for instance, dense cores that have been compressed by hot shocked stellar winds in regions of high mass star formation may not be very turbulent. Even if the turbulent pressure is comparable to the magnetic pressure, so long as the H II region is small compared to the wavelength at which the turbulent power is concentrated, a change of reference frame to one comoving with the ambient medium immediately ahead of the front maintains the applicability of our analysis. From Spitzer (1978) one finds that a D-type ionization front forms around a B1 star's H II region in a clump like those

Send offprint requests to: M.P. Redman

found by Williams et al. (1995) when the H II region's radius is only $0.07\,\mathrm{pc}\,(n_\mathrm{H}/500\,\mathrm{cm}^{-3})^{-2/3}$, which is almost certainly small compared to the aforementioned wavelength.

In Sect. 2 we describe the modifications to the jump conditions across and the propagation of IFs where there is a magnetic field in the plane of the front. We will address the more general and complex case of IF propagation at an arbitrary angle to the magnetic field in a later paper. In Sect. 3 we briefly comment on these modifications and note some of the applications of these ideas in relation to UCHIIR and other diffuse sources.

2. Model

In this first paper, we treat the simple case where the magnetic field is in the plane of the ionization front. The jump conditions are: (cf. Bertoldi & Draine 1996; Melrose 1986)

$$\rho_1 u_1 = \rho_2 u_2; \tag{1}$$

$$P_1 + \rho_1 u_1^2 + \frac{B_1^2}{8\pi} = P_2 + \rho_2 u_2^2 + \frac{B_2^2}{8\pi}; \tag{2}$$

$$B_1 u_1 = B_2 u_2; \tag{3}$$

where ρ is the gas density, u is the gas velocity in the frame of the IF, P is the pressure and B is the magnetic field strength. The subscripts 1 and 2 refer to upstream and downstream values, respectively. We define

$$c^2 = P/\rho, \quad \text{isothermal sound speed;} \tag{4}$$

$$M = \frac{u}{c}, \quad \text{Mach number;} \tag{5}$$

$$\delta = \frac{u_2}{u_1} = \frac{\rho_1}{\rho_2}, \quad \text{velocity ratio;} \tag{6}$$

$$\xi = \frac{B^2}{8\pi P} = \frac{B^2}{8\pi\rho c^2} = \frac{v_A^2}{2c^2}, \tag{7}$$

where v_A is the Alfvén speed. The parameter ξ is the reciprocal of the usual plasma parameter β. From Eqs. (1-3)

$$\frac{c_1^2(1+\xi_1)+u_1^2}{u_1} = \frac{c_2^2(1+\xi_2)+u_2^2}{u_2}. \tag{8}$$

δ is then given by

$$\mathscr{F}(\delta) = \delta^3 - \delta^2\left\{\frac{M_1^2+(1+\xi_1)}{M_1^2}\right\} + \frac{\alpha\delta}{M_1^2} + \frac{\xi_1}{M_1^2} = 0, \tag{9}$$

where $\alpha = (c_2/c_1)^2$. For the numerical calculations presented here we take $\alpha = 100$. However, lower values may be appropriate if the IF is proceeded by a dissociation front (Bertoldi & Draine 1996).

2.1. Non-magnetized ionization fronts

If $\xi_1 = 0$, Eq. (9) becomes

$$\mathscr{F}(\delta) = \delta^3 - \delta^2\left\{\frac{M_1^2+1}{M_1^2}\right\} + \frac{\alpha\delta}{M_1^2} = 0, \tag{10}$$

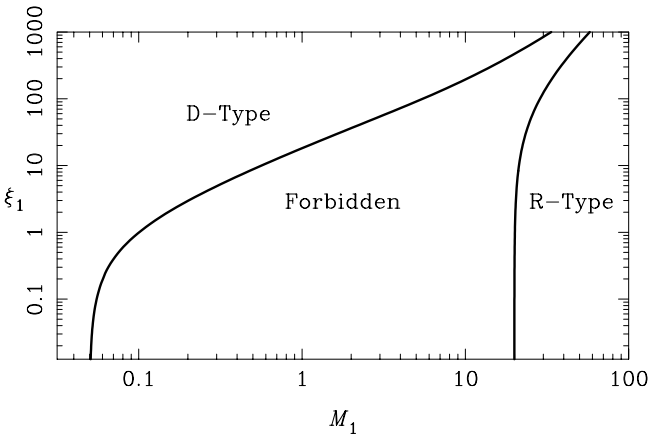

Fig. 1. ξ_1 plotted against M_1. The forbidden range of velocities decreases as the magnetic field strength increases

with (in addition to the trivial solution, $\delta = 0$) the usual solution

$$\delta = \frac{1}{2M_1^2}\left\{\left(M_1^2+1\right) \pm \left[(M_1^2+1)^2 - 4\alpha M_1^2\right]^{1/2}\right\}. \tag{11}$$

Since δ must be real, the bounds on M_1^2 which allow real solutions are $M_1^2 \gtrsim 4\alpha$ and $M_1^2 \lesssim 1/4\alpha$ giving R-type and D-type IFs respectively. For these bounds on M_1^2 there are two solution branches to δ. These are

$$M_1^2 \gtrsim 4\alpha: \quad \delta \simeq \frac{1}{2}\left\{1 \pm (1 - 2\alpha/M_1^2)\right\}, \tag{12}$$

with the positive root solution giving a weak R-type IF and the negative root solution giving a strong R-type IF. Similarly,

$$M_1^2 \lesssim 1/4\alpha: \quad \delta \simeq \frac{1}{2M_1^2}\left\{1 \pm (1 - 2\alpha M_1^2)\right\}, \tag{13}$$

the positive root solution gives a strong D-type IF and the negative root solution gives a weak D-type IF. Note that these values will also apply to the case where the magnetic field is perpendicular to the plane of the IF. There may, however, also be 'switch-on' type IFs in this case for some initial Mach numbers (cf. Draine & McKee 1993).

2.2. Magnetized ionization fronts

If $\xi_1 \neq 0$, Eq. (9) is a cubic that can have either two or zero real positive roots (since $\mathscr{F}(\delta)$ is positive at $\delta = 0$ and $\delta \to \infty$). At the boundary between these two regimes there are two coincident roots, at δ_i where $\mathscr{F}(\delta_i) = \mathscr{F}'(\delta_i) = 0$. Thus the boundary is given parametrically in terms of δ by solving these simultaneous equations for ξ_1 and M_1^2. We find

$$M_1^2 = \frac{\alpha(\delta^2+1) - 2\delta}{\delta(\delta-1)^2(\delta+2)}; \tag{14}$$

$$\xi_1 = \frac{\delta(2\alpha\delta - \delta^2 - \alpha)}{(\delta-1)^2(\delta+2)}. \tag{15}$$

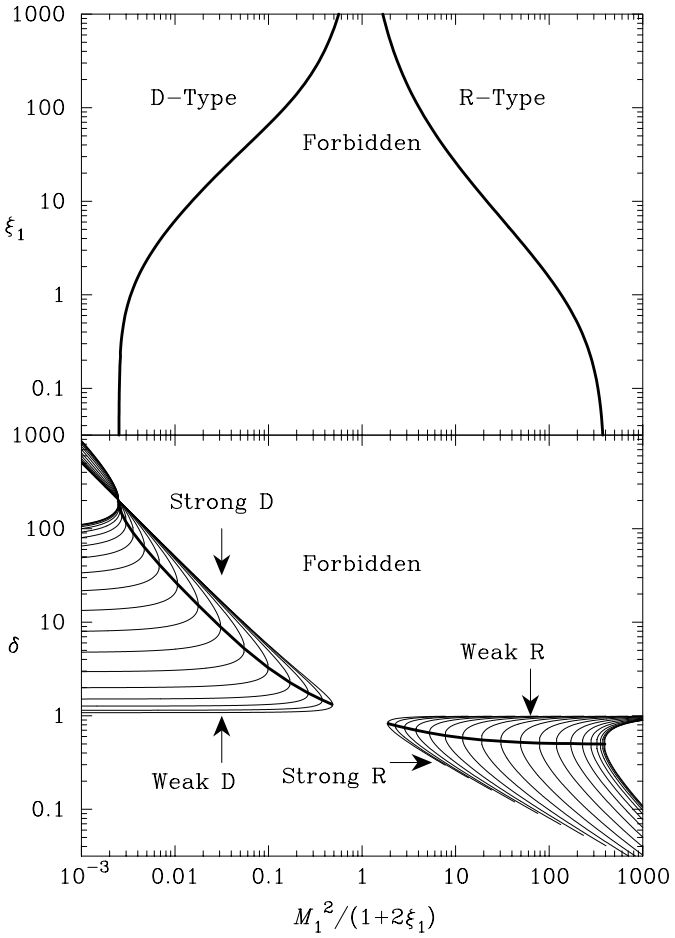

Fig. 2. Top: The ranges of ξ_1 and M_1^2 that give real solutions to Eq. 9. M_1^2 is plotted in terms of the fast mode sound speed. Bottom: The family of plots of δ as a function of M_1^2, for constant ξ_1 (thin lines). The thick line marks the critical solutions between the weak and the strong cases. This line corresponds exactly to the (ξ_1, M_1^2) plot in the top panel and can be used to judge the value of beta used for a given (δ, M_1^2) curve

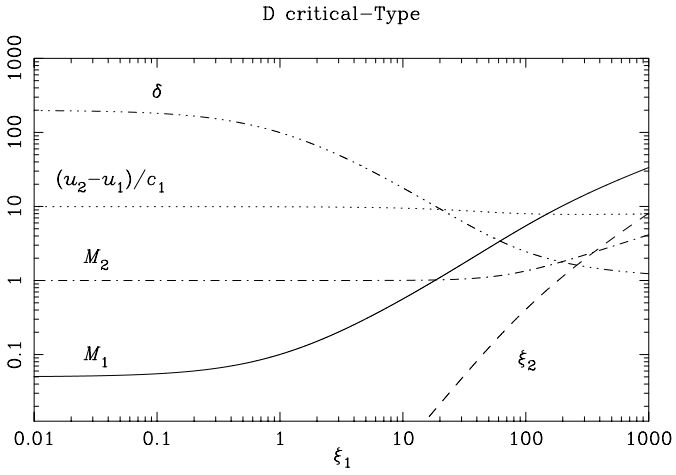

Fig. 3. Physical parameters for the D-critical IF as functions of ξ_1.

In Fig. 1 ξ_1 is plotted against M_1. The solid lines are where the two roots are coincident; the forbidden range of solutions lies in between. As $\xi \rightarrow 0$ and with $\alpha = 100$, we recover the standard non-magnetic limits of $M_1 \sim 20$ and $M_1 \sim 0.05$ for the R-type and D-type IFs respectively (Sect. 2.1). As the magnetic field strength increases, the forbidden region between the R- and D-type classes of solutions decreases significantly, which corresponds to a smaller velocity difference between the two types of IFs.

In the top panel of Fig. 2 we show the allowed and forbidden regimes for values of ξ_1 and $M_1^2/(1+2\xi_1)$, i.e. u_1 is plotted in terms of the fast mode sound speed, $(1+2\xi)^{1/2}c$. We identify the solutions with $M_1^2/(1+2\xi_1) < 1$ as being the D-type IFs and $M_1^2/(1+2\xi_1) > 1$ as being R-type IFs.

In the bottom panel of Fig. 2 we show the ranges of δ and $M_1^2/(1+2\xi_1)$ that are permitted by the presence of a magnetic field. The two solution branches, separated by the line of critical solutions, give rise to the weak and the strong IFs in the R-type and D-type zones. The standard non-magnetized ionization front solutions (Eqs. 12 and 13) are recovered at low ξ_1 and are seen as the D-type curve in the top left hand corner and the R-type curve in the bottom right hand corner.

The plots in the two panels are orthogonal to each other in (M_1^2, ξ_1, δ) space. The solid line corresponds exactly between them.

The D-critical solutions are particularly important, as they often occur at the surface of neutral clumps ablated by external ionization. In Fig. 3 we show the effects that the magnetic field will have on various parameters. The velocity ratio, δ is initially the high standard value but falls off with increasing field strength so that the velocity ratio is close to 1. The IF speed ($\propto M_1$) into the dense material increases as ξ_1 increases. The exit speed of material through the front, $u_2 - u_1$ relative to the gas immediately ahead of the front decreases slightly, from c_2 in the unmagnetized case to $\sqrt{2/3}\ c_2$ as $\xi \rightarrow \infty$. The downstream magnetic : thermal pressure ratio $\xi_2 = \xi_1/\alpha\delta$ is always less than ξ_1.

Weak R-type fronts are found in the early stages of ionization of a uniform gas distribution by a source such as a massive star. R-critical fronts mark the end of this phase. As in the non-magnetized case, strong R-type fronts are over determined (Goldsworthy 1961) and require very special circumstances for their existence. In Fig. 4 some relevant physical parameters of R-critical fronts are displayed. Significant changes occur only for $\xi_1 \gtrsim 50$. This is a high value for diffuse neutral clouds but may be expected in molecular clouds (Sect. 1). Weak R-type fronts generally evolve into D-type fronts which are affected by lower values of ξ, so that magnetic fields will play a role in this transition.

3. Conclusions

We have incorporated a plane parallel magnetic field into the continuity equations across an ionization front. Significant dif-

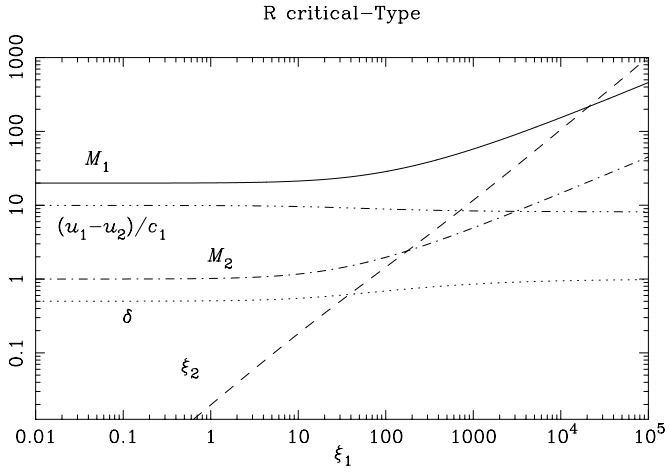

Fig. 4. Physical parameters for the R-critical IF as functions of ξ_1.

ferences arise between the magnetized and non-magnetized cases. The velocity difference between the R-type and the D-type is greatly reduced. Furthermore, the propagation speed of the important D-critical class of IF is increased with respect to the material immediately ahead of the front. This is likely to have important consequences for the mass loss rates and lifetimes of dense neutral clumps exposed to ionizing radiation from a massive star. A detailed calculation will include a self-consistent treatment of the density and temperature structure of the clump and the ionizing flux to which it is exposed. It must also account for the effects on the conditions upstream from the front which may be modified by the passage of a preceding hydromagnetic shock. In future papers we will address the structure of the magnetized fronts for arbitrarily inclined magnetic fields, the evolution of H II regions driven into magnetic media and the effects of magnetization on clump mass loss rates.

Acknowledgements. This work was supported by PPARC through Graduate Studentships (MPR, BRF) and a Standard Grant Research Associateship (RJRW). JED is grateful to the Australian National University Theory Centre for support of a visit during which part of this work was carried out. An anonymous referee made thoughtful comments.

References

Axford W. F., 1961, Phil. Trans. R. Soc. London Ser. A 253, 301
Bertoldi F., Draine B. T., 1996, ApJ 458, 222
Bertoldi F., McKee C. F., 1990, ApJ 354, 529
Draine B. T., McKee C. F., 1993, ARA&A 31, 373
Dyson J. E., 1968, Ap&SS 1, 388
Dyson J. E., 1994, in Star Formation & Techniques in Infrared & mm-Wave Astronomy, T. P. Ray & S. V. W. Beckwith (eds). Proceedings of the Berlin EADN Summer School, Springer-Verlag (Berlin) p. 93
Dyson J. E., Hartquist T. W., Williams R. J. R., Redman M. P., 1997, in The Interaction of Stars with Their Environment, V. Tóth (ed). Proc. Konkoly Observatory Budapest, in press
Dyson J. E., Williams R. J. R., Redman M. P., 1995, MNRAS 277, 700
Goldsworthy F. A., 1961, Phil. Trans. R. Soc. London Ser. A 253, 277
Hartquist T. W., Dyson J. E., 1993, QJRAS 34, 57
Hester J. J., Scowen P. A., Sankritt R., et al., 1996, AJ 111, 2349
Kahn F. D., 1954, Bull. Astron. Inst. Neth. 12, 187
Kahn F. D., 1969, Physica 41, 172
Lizano S., Cantó J., 1995, Rev. Mex. Astron. y Astro. Series de Conferencias 1, 29
Lizano S., Cantó J., Garay G., Hollenbach D., 1996, ApJ 468, 739
Melrose D. B., 1986, Instabilities in Space and Laboratory Plasmas. Cambridge University Press
Myers P. C., Goodman A. A., Gusten R., Heiles C., 1995, ApJ 442, 177
Myers P. C., Khersonsky V. K., 1995, ApJ 442, 186
O'Dell C. R., Handron K. D., 1996, AJ 111, 1630
Redman M. P., Williams R. J. R., Dyson J. E., 1996, MNRAS 280, 661
Spitzer L., 1978, Physical Processes in the Interstellar Medium. John Wiley & Sons
Williams J. P., Blitz L., Stark A. A., 1995, ApJ 451, 252
Williams R. J. R., Dyson J. E., Redman M. P., 1996, MNRAS 280, 667
Yorke H. W., 1986, ARA&A 24, 49

This article was processed by the author using Springer-Verlag LaTeX A&A style file *L-AA* version 3.